

Received April 4, 2021, accepted May 19, 2021, date of publication May 24, 2021, date of current version June 2, 2021.

Digital Object Identifier 10.1109/ACCESS.2021.3083285

# Compound Speckle Reduction in Laser Imaging Systems by Using a Vibrating Multimode Fiber and a Tracked Moving Flexible DOE Loop

JUN ZHOU<sup>1,2</sup>, ZICHUN LE<sup>1</sup>, ZONGSHEN LIU<sup>1</sup>, YANXIN DAI<sup>1</sup>,  
YANYU GUO<sup>1</sup>, JIAYU DENG<sup>1</sup>, AND JIAPU LI<sup>1</sup>

<sup>1</sup>College of Science, Zhejiang University of Technology, Hangzhou 310023, China

<sup>2</sup>College of Engineering Training Center, China Jiliang University, Hangzhou 310018, China

Corresponding author: Zichun Le (lzc@zjut.edu.cn)

This work was supported by the National Natural Science Foundation of China under Grant 61975183.

**ABSTRACT** The speckle phenomenon produced by coherent waves interfering with each other is undesirable in laser imaging systems. For each of the laser speckle reduction methods in the literature, it is difficult to reduce speckle to an extremely low level (<3%) and also ensure good image quality. Therefore, a compound speckle reduction method based on the combination of a vibrating multimode fiber and a tracked moving flexible DOE loop is proposed and demonstrated for the first time. We have experimentally demonstrated the effectiveness of the proposed compound method, which can reduce the speckle contrast to 1.96% and obtain good spot quality. The relationship between the time-averaging effect of the speckle patterns from a vibrating multimode fiber and from a tracked moving DOE loop is discussed thoroughly. Our experimental results are in good agreement with Goodman's speckle theory. We expect that the compound speckle reduction method we proposed will have promising potential for applications in laser imaging systems.

**INDEX TERMS** Flexible DOE loop, laser imaging systems, multimode fiber, speckle reduction.

## I. INTRODUCTION

Lasers have been widely used in various imaging systems, such as in projection displays and medical imaging, due to their advantages of high brightness, a wide color gamut, high directionality, and a long lifetime [1]–[3]. However, the propagation or reflection of a highly coherent laser through an optically rough object causes interference for the scattered light, which results in a random light intensity distribution, known as granular speckles [4], [5]. Speckles degrade the quality of images; therefore, reducing laser speckle has become an urgent task.

Numerous methods have been developed for speckle reduction in laser imaging systems [6]–[30]; according to the different mechanisms of speckle reduction, those methods can generally be divided into two categories: one involves reducing the coherence of the laser, and the other is based on speckle averaging by creating many uncorrelated independent dynamic speckle patterns.

The associate editor coordinating the review of this manuscript and approving it for publication was Kin Kee Chow.

The methods to reduce laser coherence include wavelength diversity, polarization diversity and angle diversity. For wavelength diversity, the use of laser diode arrays or a broadband laser is usually required to reduce speckles [6]–[8]; this increases the cost and complexity of light sources. The use of polarization diversity to reduce speckles is generally limited because lasers have only two polarization states [9]. Angular diversity is one of the most effective techniques, and speckle reduction can be achieved by a diffractive optical element (DOE), diffuser, multimode fiber, light pipe, etc. [10]–[16]. Using a static DOE or diffuser can only produce a finite number of diffracted subbeams, and its speckle reduction ability is insufficient. To use a static multimode optical fiber or a light pipe to reduce speckles completely, a sufficient length (approximately a few hundred meters) and a large numerical aperture are required [17], [18].

Speckle noise can also be reduced on average by creating many uncorrelated independent dynamic speckle patterns. Usually, such methods can be achieved by fast vibrating or rotating the screen [19], by projecting a moving DOE or diffuser with phase distribution on the screen [20], [21],

by vibrating a multimode optical fiber [22]–[24], or by using other time-varying components such as liquid crystal on silicon (LCOS) [25]. Screen movement is not preferable for laser imaging systems, which require large shifts to reduce speckle noise. The use of a DOE or other moving optical elements, as reported in the literature [26]–[28], requires mechanical movements, and it increases device volume and power consumption. For the time-varying optical component (LCOS), its response time is long, and it cannot produce enough independent speckle patterns during the time resolution of the human eye.

Recently, our group proposed a flexible DOE loop based on pseudorandom binary sequences with tracked motion, which can effectively suppress speckles in the entire visible spectrum and reduce the device size in laser imaging systems [29]. This proposed method is based on concurrent mechanisms, which are the angle diversity caused by the diffraction of the DOE structure and the speckle time-averaging effect with the tracked motion of the DOE loop. The material used for the flexible DOE loop is polypropylene (PP), which has good optical performance and machining properties. Once the parameters of the DOE loop are optimized and determined, the mask can be made by photolithography and electroplating, and finally, mass production can be achieved by hot pressing. Therefore, the manufacturing process is relatively easy and convenient. However, although the resulting speckle contrasts were as low as 2.8% when using a tracked moving flexible DOE loop, the imaging quality was not very good because we did not use a laser with high coherence and good beam quality as the light source of the imaging system [30].

When a laser with high coherence and good beam quality is used as the light source, the imaging quality should be greatly improved, but high coherence inevitably leads to high speckle contrast. In this case, it is difficult to reduce speckles to a low level in the whole visible band if only a tracked moving flexible DOE loop is used. For this reason, a compound speckle reduction method combining a vibrating multimode fiber and a tracked moving flexible DOE loop is proposed in the present paper. When a multimode fiber is vibrated, it can not only support the propagation of hundreds of waveguide modes to introduce angle diversity but also generate multiple dynamic speckle patterns to average during the time resolution of the human eye. Therefore, the vibration of a multimode fiber can be regarded as a means to manipulate the coherence of the laser light source from highly coherent to partially coherent light, which can reduce the speckle contrast and ensure good image quality.

According to Goodman's speckle theory [4], [5], each speckle reduction effect from the compound speckle reduction method may be viewed as introducing a certain number of degrees of freedom. If we have  $r$  independent mechanisms for introducing new degrees of freedom, then the total number  $R$  of degrees of freedom is simply  $R = \prod_{r=1}^R R_r$ , and the total contrast of the objective speckle is as follows:  $C_{obj} = 1/\sqrt{R}$ . However, there have been few experiments

to verify the effectiveness of a compound speckle reduction method.

The proposed compound speckle reduction method combining a vibrating multimode fiber and a tracked moving flexible DOE loop is investigated in this paper. We first briefly introduce the theoretical methods of speckle reduction with a vibrating multimode fiber and with a tracked moving flexible DOE loop. Then, we experimentally demonstrate the effectiveness of the proposed compound method, with which the speckle contrast can be reduced to 1.96%. The effects on the speckle contrast with both stationary a multimode fiber and a DOE loop with a vibrating multimode fiber only, with a rotating DOE loop only, and with a vibrating multimode fiber and a rotating DOE loop together are shown and discussed in our experiments. The relationship between the time-averaging effect of the vibrating multimode fiber and the time-averaging effect of the tracked moving DOE loop is discussed in detail. Our experimental results agree well with Goodman's speckle theory. We believe that the proposed compound speckle reduction method will have promising applications in speckle-free laser imaging systems.

## II. THEORETICAL BACKGROUND

### A. SPECKLE REDUCTION THEORY OF A VIBRATING MULTIMODE FIBER

When a coherent laser beam is coupled to a stationary multimode fiber, speckle forms at the exit end of a multimode fiber due to the interference among the guided modes. For a multimode fiber with a given numerical aperture ( $NA$ ), the use of a long fiber increases the fiber mode delay difference, and the laser speckle can be reduced to a certain level. The speckle contrast ( $C$ ) at the end of the multimode fiber with different fiber lengths  $L$  can be calculated as follows [14]:

$$C(L) = \left[ 1 + 0.5 (2\pi \Delta v)^2 \times \frac{\delta\tau^2}{3} \right]^{-1/4}, \quad \delta\tau = \frac{L(NA)^2}{2nc} \quad (1)$$

where  $\Delta v$  represents the Gaussian spectral profile with a  $1/e$  half-width,  $\delta\tau$  is the maximum time difference between the first-to-arrive and last-to-arrive light wave modes,  $n$  is the refractive index of the fiber core, and  $c$  is the speed of light in a vacuum.

Assuming that there are  $M$  guided modes propagating in a multimode fiber, the complex amplitude field at the fiber output can be expressed as:

$$A(x, y) = \sum_{m=1}^M a_m(x, y) \exp[j\phi_m(x, y)] \quad (2)$$

where  $a_m$  and  $\phi_m$  stand for the amplitude and phase distribution of the  $m$ th mode, respectively,  $\phi_m = \beta_m L + \varphi_m$ ,  $\beta_m$  and  $\varphi_m$  are the propagation constant and random phase shift of the  $m$ th mode, respectively. Thus, the intensity of the light output at the fiber facet can be written as:

$$I(x, y) = \sum_{m=1}^M \sum_{n=1}^M a_m a_n \exp\{j[(\beta_m - \beta_n)L + \varphi_m - \varphi_n]\} \quad (3)$$

The quantitative measure of speckle on the fiber end is obtained by the speckle contrast. It is defined as the ratio of the standard deviation to the mean of the intensity [4], [5]:

$$C = \frac{\sigma_I}{\langle I(x, y) \rangle} = \sqrt{\frac{\langle I(x, y)^2 \rangle - \langle I(x, y) \rangle^2}{\langle I(x, y) \rangle^2}} \quad (4)$$

The output speckle intensity at the end of the fiber is very sensitive to external vibration. When the multimode fiber is vibrated, two mechanisms occur: phase modulation and mode coupling [31]. The phase modulation in the multimode fiber is the change in the optical phase caused by the change in both the fiber length ( $L$ ) and the refractive index ( $n$ ), which can be expressed as:

$$\frac{\partial \phi_m}{\beta_m L} = \left( \frac{1}{L} \times \frac{\partial L}{\partial F} + \frac{1}{n} \times \frac{\partial n}{\partial F} \right) \times \delta F \quad (5)$$

where  $\delta F$  is the transient vibration signal applied to the fiber. It can be seen from (5) that phase modulation is common for all fiber modes and that there is no energy exchange between modes. The phase modulation is caused by the external vibration signal, which is then converted to the subsequent intensity modulation over the multimode fiber. If the change in the intensity modulation is faster than the resolution time of the human eye, the speckle contrast can be effectively reduced by averaging the speckle intensity.

Another mechanism is that coupling occurs between the guided modes when a multimode fiber is vibrated. The variation in the power of the  $m$ th mode can be expressed as:

$$\Delta P_m = \sum_{n=1}^M h_{mn}(P_m - P_n) \quad (6)$$

where  $P_m$  and  $P_n$  represent the initial power of the  $m$ th and  $n$ th modes, respectively.  $M$  is the total number of guided modes, and  $h_{mn}$  is the coupling coefficient between modes  $m$  and  $n$ . If the change rate of the coupling coefficient  $h_{mn}$  is increased in a random manner by external vibration, the average power of the speckle intensity is increased and the speckle contrast is reduced.

### B. SPECKLE REDUCTION THEORY OF THE TRACKED MOVING FLEXIBLE DOE LOOP

It has been shown that the application of a moving DOE can not only generate multiple diffraction orders for angle diversity but also generate the time-varying speckle patterns; thus the speckle contrast can be effectively reduced [32]. In general, the application of one-dimensional (1D) DOE provides a comparatively small effect in speckle reduction. The approximate estimated speckle contrast is expressed as [33]:

$$C_{1D} \approx \sqrt{\frac{2}{9N_{code}}} \quad (7)$$

where  $N_{code}$  is the code length of a pseudorandom binary sequence in a single period of the DOE. It has been demonstrated that the usage of two-dimensional (2D) DOE is more effective in speckle reduction than 1D DOE. A simplified

formula for the speckle contrast of a 2D DOE with code length  $N_{code}$  is given as [34]:

$$C_{2D} = C_x C_y \approx \frac{2}{(3\sqrt{3}N_{code})} \quad (8)$$

The flexible DOE loop with tracked motion can be regarded as a dynamic 2D DOE structure in real time by overlapping a double-sided moving 1D DOE. The DOE loop we made is composed of three 1D-DOE parts with different inclination angles ( $45^\circ - \Delta\varphi$ ,  $45^\circ$ ,  $45^\circ + \Delta\varphi$ ,  $\Delta\varphi \ll 45^\circ$ ), which are rolled up in a loop. The 1D-DOE structure is a periodic  $M$  sequence code that has a code length of  $N_{code}$  and a period  $T_0 = N_{code} \times T$  with elementary unit width  $T$ . When the DOE loop moves around the rotating spindle in a tracked motion by the motor, three groups of different inclination pairs appear in the front and back of the DOE loop. After the laser beam passes through the DOE loop, the speckle contrast can be effectively reduced by angle diversity and by averaging multiple different speckle patterns during the time resolution of the human eye. The detailed theoretical analysis and derivation can be found in our previous publications [30], [35].

### III. EXPERIMENTAL SETUP

First, to evaluate speckle reduction efficiency using a vibrating multimode fiber, it is necessary to measure the speckle contrast of the screen image illuminated by laser beam through the vibrating fiber. The exit end of the fiber should be placed in the optical plane conjugate to the screen to obtain an image of fiber end on the screen. Fig. 1 shows the experimental setup for measuring the speckle reduction efficiency using a vibrating multimode fiber. In the experiment, we used a step-index multimode fiber with a core diameter of 1 mm, fiber length of  $L = 2$  m, and numerical aperture of 0.37. In Fig. 1,  $S_1$ ,  $S_2$ ,  $S_3$ ,  $S_4$  and  $S_5$  are the distance from the convergent lens to the incident end of the fiber, from the exit end of the fiber to the objective lens, from the objective lens to the screen, from the screen to the camera lens and from the camera lens to the photodiode array, respectively.  $D_1$ ,  $D_2$ ,  $D_3$ , and  $D_4$  represent the aperture of the diaphragm, the lens that converges and couples light into the incident end of the fiber, the objective lens, and the camera lens, respectively. The vibrator is a self-made loud speaker-based modulator, and a segment of the fiber is fixed on the vibrator, which is driven by the controller, so that the multimode fiber is forced into vibration. We can change the input numerical aperture of the laser beam by adjusting the diameter of diaphragm  $D_1$  to excite the multiple propagation modes in the multimode fiber for speckle reduction.

Fig. 2 shows the experimental setup for measuring the speckle reduction efficiency using the combination of a vibrating multimode fiber and a tracked moving flexible DOE loop. The difference from Fig. 1 is that partially despeckled light emerging from a vibrating multimode fiber is then incident on the moving flexible DOE loop. The DOE loop used in

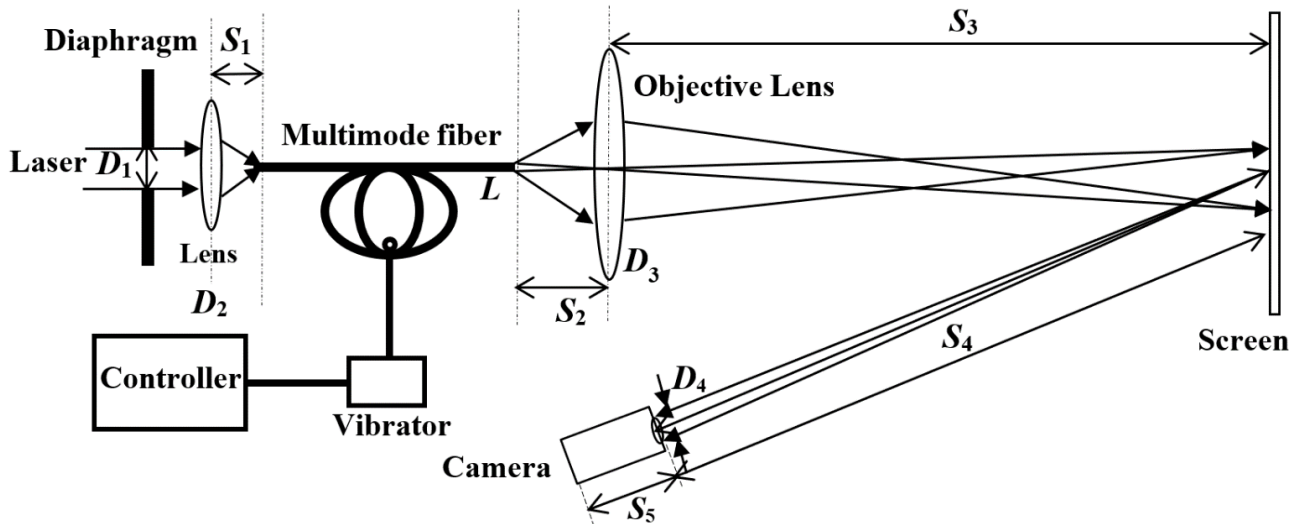


**FIGURE 1.** Experimental setup for measuring the speckle reduction efficiency using a vibrating multimode fiber.  $D_1 = 15.18\text{mm}$ ,  $S_1 = 60\text{mm}$ ,  $D_2 = 25\text{mm}$ ,  $S_2 = 62\text{mm}$ ,  $D_3 = 51\text{mm}$ ,  $S_3 = 1500\text{mm}$ ,  $D_4 = 1\text{mm}$ ,  $S_4 = 2100\text{mm}$ , and  $S_5 = 25\text{mm}$ .

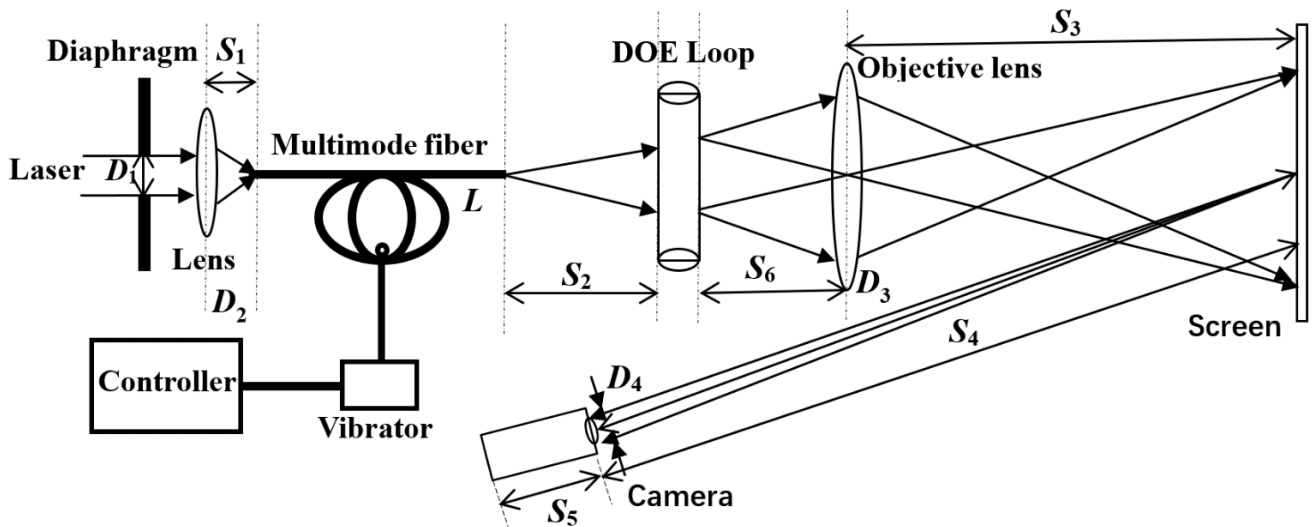


**FIGURE 2.** Experimental setup for measuring the speckle reduction efficiency using the combination of a vibrating multimode fiber and a tracked moving flexible DOE loop.  $D_1 = 10.5\text{mm}$ ,  $S_1 = 60\text{mm}$ ,  $D_2 = 25\text{mm}$ ,  $S_2 = 85\text{mm}$ ,  $D_3 = 51\text{mm}$ ,  $S_3 = 1500\text{mm}$ ,  $D_4 = 1\text{mm}$ ,  $S_4 = 2100\text{mm}$ ,  $S_5 = 25\text{mm}$ , and  $S_6 = 62\text{mm}$ .

our experiment is composed of the three 1D-DOE parts with different inclination angles, which in turn are  $44^\circ$ ,  $45^\circ$ , and  $46^\circ$ . The 1D-DOE structure is a periodic  $M$  sequence code that has a code length of  $N_{\text{code}} = 15$  and a period  $T_0 = N_{\text{code}} \times T$  with an elementary unit width of  $T = 4\mu\text{m}$ . The DOE structure depth is  $530\text{nm}$  to ensure effective speckle reduction in the visible light range. The laser beam from the DOE loop is projected to the screen through the objective lens, and a camera is used to capture the picture of the light spot on the screen to evaluate the speckle contrast. The camera objective lens has a focal length of  $S_5 = 25\text{mm}$ , the diameter of the input diaphragm of camera is  $D_4 = 1\text{mm}$ , and the photodiode has a transverse size of  $5.8\mu\text{m}$ . For accurate evaluation of the speckle contrast, we select the five different positions in

the image captured by the camera to calculate the mean and standard deviation of the intensity.

#### IV. EXPERIMENTAL RESULTS AND DISCUSSION

##### A. SPECKLE REDUCTION WITH A VIBRATING MULTIMODE FIBER

To verify the speckle reduction efficiency of a vibrating multimode fiber, we use a green laser and a red laser as the sources of coherent illumination in Fig. 1. Green ( $\lambda = 520\text{nm}$ ), and Red ( $\lambda = 640\text{nm}$ ) lasers were used in the experiments, and the linewidth of both lasers are rough approximation as  $2\text{nm}$ . The vibrator is driven at a frequency of  $400\text{Hz}$ , and the voltage is set at  $1\text{VPP}$  (peak to peak). The camera exposure time is set to  $60\text{ms}$  for all the measurements.

**TABLE 1.** The speckle patterns and their 1D Intensity distributions are shown when the laser light passes through the static multimode fiber and the laser light passes through the vibrating multimode fiber for green and red lasers.

Green Laser + Static multimode fiber ( $C_1$ )	Green Laser +Vibrating multimode fiber ( $C_2$ )	Speckle reduction Coefficient induced by vibration ( $C_1/C_2$ )
<p style="text-align: center;"><math>C_1=8.93\%</math></p>	<p style="text-align: center;"><math>C_2=4.62\%</math></p>	$C_1/C_2=1.93$
<p style="text-align: center;">Distance(pixels)</p>	<p style="text-align: center;">Distance(pixels)</p>	
Red Laser + Static multimode fiber ( $C_3$ )	Red Laser +Vibrating multimode fiber ( $C_4$ )	Speckle reduction Coefficient induced by vibration ( $C_3/C_4$ )
<p style="text-align: center;"><math>C_3=19.60\%</math></p>	<p style="text-align: center;"><math>C_4=9.24\%</math></p>	$C_3/C_4=2.12$
<p style="text-align: center;">Distance(pixels)</p>	<p style="text-align: center;">Distance(pixels)</p>	

First, the initial speckle contrast values of the green and red laser lights are tested to be 39.38% and 53.49%, respectively. Then, the speckle patterns and their 1D intensity distributions are shown in Table 1 when the laser light passes through the static multimode fiber and the laser

light passes through the vibrating multimode fiber for the green and the red lasers. The speckle contrast value is shown in the upper right corner of each speckle pattern. 1D intensity distribution is extracted from the red dashed line.

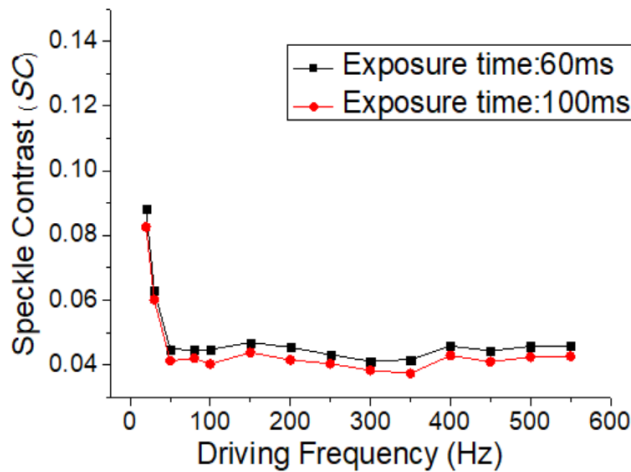


**FIGURE 3.** The relationship between speckle contrast and driving frequency when the camera exposure time is 60 ms and 100 ms, respectively.

When the laser light passes through a static multimode fiber with a length of 2 m, the speckle contrast is first reduced. However, the speckle contrast value does not fit well with (1) and is usually larger. The reason is that the speckle in the image on the screen is a compound speckle, which includes not only the objective speckle due to mode interference in a static multimode fiber but also the subjective speckle due to the light scattering on the screen. When the vibration is applied to the multimode fiber, the speckle contrast of output patterns can be further reduced, which can be clearly seen from the magnitude of the 1D intensity fluctuation before and after the vibration in Table 1. The speckle reduction coefficient is different for the green laser ( $C_1/C_2 = 1.93$ ) and red laser ( $C_3/C_4 = 2.12$ ) because the spectrum of the green laser is slightly wider than that of the red laser used in the experiment, which makes the initial speckle contrast of the green laser smaller than that of the red laser.

When the vibration is applied to the multimode fiber, the speckle contrast of the green laser is only 4.62%. Compared with the red laser, the objective speckle value of the green laser is closer to the subjective speckle value. The compound speckle in the image on the screen is clamped by the subjective speckle, so the speckle reduction coefficient of the green laser is smaller than that of the red laser.

Since the drive voltage of the vibrator we used is at most 1 VPP and the driving frequency is adjustable, the effect of the driving frequency on speckle reduction is also investigated. The relationship between speckle contrast and driving frequency is shown in Fig. 3 when the camera exposure time is 60ms and 100 ms, respectively.

The laser used is a green laser, and the driving frequency varies from 20 Hz to 550 Hz. As shown in Fig. 3, as the driving frequency increases to approximately 50 Hz, the speckle contrast decreases rapidly. When the driving frequency is greater than 50 Hz, the speckle contrast is in the small fluctuation range. There is a slight difference in speckle contrast between exposure times of 60 ms (black curve) and 100ms

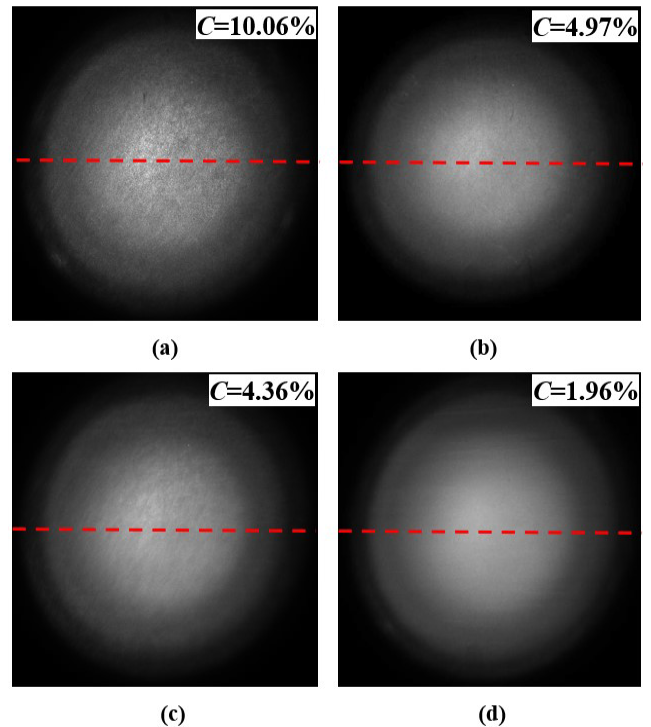


**FIGURE 4.** The speckle patterns captured by the camera for four different states. (a) Both the multimode fiber and the DOE loop are stationary, (b) the multimode fiber is vibrated and the DOE loop is stationary, (c) the multimode fiber is stationary and the DOE loop is rotated, (d) the multimode fiber is vibrated and the DOE loop is rotated.

(red curve). This can be explained by the fact that the mechanism of speckle reduction by a vibrating multimode fiber forms different speckle patterns, which are then averaged during the exposure time of the camera. When the exposure time is longer, more speckle patterns can be generated, and the speckle contrast is lower. The driving frequency should be greater than the reciprocal of the exposure time to use all different speckle patterns during one period of vibration. Therefore, we choose the driving frequency of the vibrator greater than 50Hz based on the experimental results shown in Fig. 3.

**B. THE COMPOUND SPECKLE REDUCTION METHOD**

In this section, the compound speckle reduction method by the combination of a vibrating multimode fiber and a tracked moving flexible DOE loop is presented. The optical scheme for speckle reduction using the proposed method has been shown in Fig. 2.

Fig. 4 shows the speckle patterns captured by the camera with four different states: (a) both the multimode fiber and the DOE loop are stationary, (b) the multimode fiber is vibrated and the DOE loop is stationary, (c) the multimode fiber is stationary and the DOE loop is rotated, and (d) the multimode fiber is vibrated and the DOE loop is rotated. When the multimode fiber is vibrated, the vibrator is driven at a frequency of 400Hz, and the voltage is set at 1 VPP. When the DOE loop is rotated, the motor speed is set to 16.7 mm/s. In the

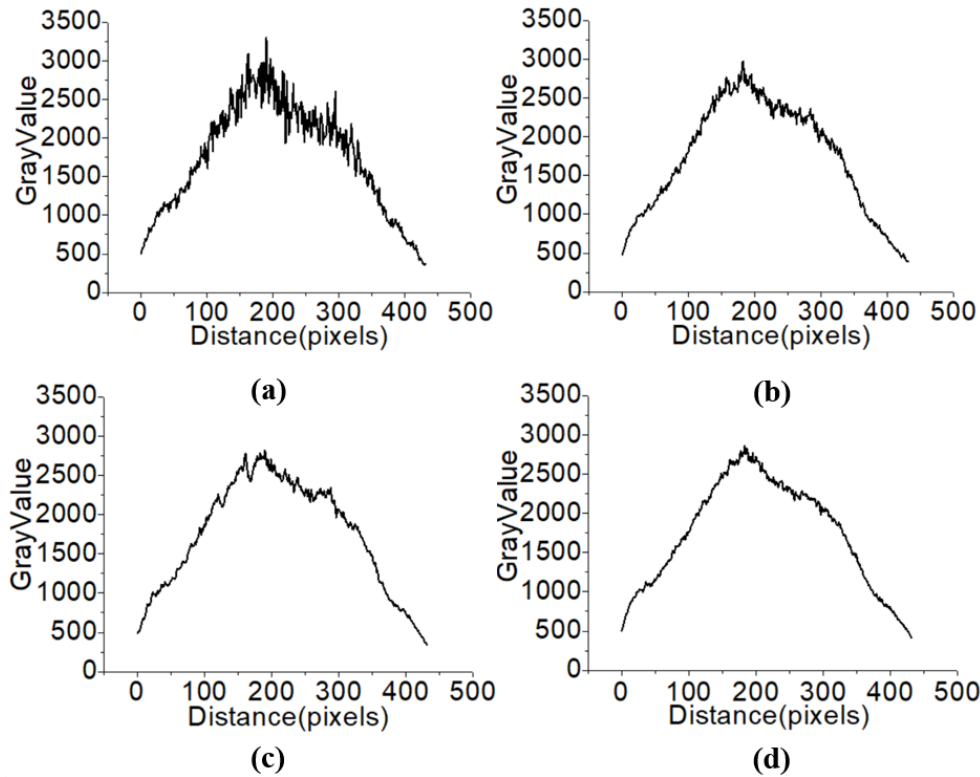


**FIGURE 5.** The 1D intensity distributions of speckle patterns, corresponding to the ones in Fig. 4, are shown for four different states. (a) Both the multimode fiber and the DOE loop are stationary, (b) the multimode fiber is vibrated and the DOE loop is stationary, (c) the multimode fiber is stationary and the DOE loop is rotated, (d) the multimode fiber is vibrated and the DOE loop is rotated. The light intensity distributions are extracted from the red dashed line shown in Fig. 4.

experiments, a green laser is used, and the camera exposure time is set to 100 ms for all the measurements.

It can be found from Fig. 4 that a reduction in speckle contrast is achieved when the multimode fiber is vibrated and the DOE loop is stationary, which is approximately the same as the reduction in speckle contrast achieved when the multimode fiber is stationary and the DOE loop is rotated. Therefore, the vibrating multimode fiber and the rotating DOE are both very effective in the speckle reduction. Moreover, the maximum speckle reduction is achieved by combining a vibrating multimode fiber and a rotating DOE loop. Therefore, a laser imaging system with extremely low speckle contrast (the speckle contrast is 1.96%) can be achieved with the proposed compound speckle reduction method.

The 1D intensity distributions are plotted in Fig. 5 for each of the corresponding speckle patterns shown in Fig. 4. The light intensity distributions are extracted from the red dashed line shown in Fig. 4.

As can be seen from Fig. 5, the intensity fluctuation is significantly decreased when the multimode fiber is vibrated and the DOE loop is rotated as compared to when both the multimode fiber and the DOE loop are stationary. The above results further indicate that the proposed compound speckle reduction method by the combination of a vibrating multimode fiber and a tracked moving flexible DOE loop is feasible and effective.

### C. DISCUSSION

There are multiple speckle formation mechanisms in our experimental setup, as shown in Fig. 2. It is assumed that the speckle formation mechanisms before the objective lens belong to the objective speckle and that the speckle caused by screen scattering is the subjective speckle. The compound speckle on the screen captured by the camera can be written as follows [14]:

$$C = \sqrt{\frac{R+K}{2RK}} = \frac{1}{\sqrt{2}} \sqrt{\frac{1}{R} + \frac{1}{K}} \quad (9)$$

where the factor 2 is introduced by the two independent orthogonal polarizations,  $R$  represents the total degree of objective speckle reduction freedom, and  $K$  is the subjective speckle reduction freedom. The value of  $K$  can be simply calculated when the objective lens is almost filled [5]:

$$K = \frac{\Omega_p}{\Omega_i} = \left( \frac{D_3}{2S_3} \right)^2 = \left( \frac{S_4 D_3}{S_3 D_4} \right)^2 = \left( \frac{2100 \times 51}{1500 \times 1} \right)^2 = 5098 \quad (10)$$

where  $\Omega_p$  is the solid angle subtended by the objective lens aperture  $D_3 = 51$  mm and  $\Omega_i$  is the solid angle subtended by the camera lens aperture  $D_4 = 1$  mm, with both solid angles measured from the screen.  $S_3 = 1500$  mm and  $S_4 = 2100$  mm

**TABLE 2. Characteristics of the speckle reduction methods for their comparison and evaluation.**

Characteristics	Compound method based on a vibrating multimode fiber and a tracked moving flexible DOE loop	Tracked moving flexible DOE loop only [29]	Combination of micro-scanning mirrors and multimode fibers [37]	Colloidal solution with dispersed particles [38]
Speckle contrast value (%)	1.96%	3.9%	7.94%	3.4%
System size	++	+	++	+++
Power consumption	++	+	++	-
Complexity of optics and electronics	++	+	++	+++
Manufacturing cost	++	+	++	+++

are the distances from the objective lens to the screen and from the screen to the camera lens, respectively.

According to (9), the total degree of objective speckle reduction freedom can be obtained as follows:

$$R = \frac{1}{2C^2 - \frac{1}{K}} \tag{11}$$

The total degree of objective speckle reduction freedom from the four states in Fig. 4 can be calculated by the speckle contrast from the experimental data and the calculated  $K$  value in (10):

$$R_{(a)} = \frac{1}{2C_{(a)}^2 - \frac{1}{K}} = \frac{1}{2 \times (0.1226)^2 - \frac{1}{5098}} = 33.5 \tag{12a}$$

$$R_{(b)} = \frac{1}{2C_{(b)}^2 - \frac{1}{K}} = \frac{1}{2 \times (0.0497)^2 - \frac{1}{5098}} = 210.8 \tag{12b}$$

$$R_{(c)} = \frac{1}{2C_{(c)}^2 - \frac{1}{K}} = \frac{1}{2 \times (0.0436)^2 - \frac{1}{5098}} = 277.3 \tag{12c}$$

$$R_{(d)} = \frac{1}{2C_{(d)}^2 - \frac{1}{K}} = \frac{1}{2 \times (0.0196)^2 - \frac{1}{5098}} = 1747.7 \tag{12d}$$

The physical meaning of (12a) can be interpreted as the degree of speckle reduction freedom for the angle diversity of a static multimode optical fiber and a static DOE loop. Reference [36] shows that angle diversity and speckle time-averaging effects are two independent speckle reduction mechanisms obtained by introducing new degrees of freedom. When the multimode fiber is vibrated and the DOE loop is stationary, the degree of speckle reduction freedom for the time-averaging effect of the vibrating multimode fiber is calculated as:

$$R_1 = \frac{R_{(b)}}{R_{(a)}} = \frac{210.8}{33.5} = 6.3 \tag{13a}$$

Similarly, the degree of speckle reduction freedom for the time-averaging effect of the rotating DOE loop is calculated

as:

$$R_2 = \frac{R_{(c)}}{R_{(a)}} = \frac{277.3}{33.5} = 8.3 \tag{13b}$$

The degree of speckle reduction freedom for the time-averaging effect of the vibrating fiber and the tracked moving DOE loop is calculated as:

$$R_3 = \frac{R_{(d)}}{R_{(a)}} = \frac{1747.7}{33.5} = 52.2 \tag{13c}$$

Therefore, the total degree of compound objective speckle reduction freedom for the time-averaging effect is equal to the product of the speckle reduction degree of each method, i.e.,  $R_3 \approx R_1 \times R_2$  ( $52.2 \approx 6.3 \times 8.3$ ). This is well confirmed by the calculated result of the compound objective speckle reduction degrees of freedom according to Goodman’s speckle theory mentioned in the seventh paragraph of the Introduction Section.

The main characteristics of the speckle reduction methods for comparison and evaluation purposes are summarized in Table 2. It mainly includes the following four schemes:

- 1) Compound method based on a vibrating multimode fiber and a tracked moving flexible DOE loop;
- 2) Tracked moving flexible DOE loop only [29];
- 3) Compound method based on a micro-scanning mirrors and multimode fibers [37];
- 4) Colloidal solution with dispersed particles [38].

The number of plus signs qualitatively indicates the value of the considered characteristic for a particular speckle reduction method. Less speckle contrast values with fewer plus signs are obviously preferable. In the case of a comprehensive consideration of speckle contrast and other parameters such as system size, power consumption, complexity and manufacturing cost [39], [40], our proposed compound speckle reduction method based on the combination of a vibrating multimode fiber and a tracked moving flexible DOE loop is relatively superior, and thus has significant advantages in reducing speckles in laser imaging systems.



## V. CONCLUSION

In this study, the speckle reduction method by a vibrating multimode fiber was first experimentally investigated. When a multimode fiber is vibrated, the speckle pattern changes due to phase modulation and mode coupling, and the speckle contrast can be reduced by angle diversity and the time averaging of the speckle patterns. The influence of the vibration frequency on the speckle reduction was also analyzed. Moreover, further speckle reduction was achieved by the combination of a vibrating multimode fiber and a tracked moving flexible DOE loop. This reduces the speckle contrast to 1.96%, which is extremely low and cannot be perceived by human vision. Meanwhile, a laser with high coherence can be used with the proposed compound speckle reduction method to obtain the higher imaging quality. Therefore, we expect that the compound speckle reduction method we proposed will show good performance and high efficiency in applications related to laser imaging systems.

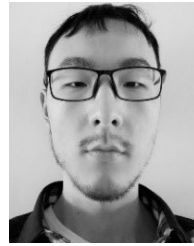
## ACKNOWLEDGMENT

The authors would like to thank Dr. A. Lapchuk for the valuable discussions.

## REFERENCES

- [1] M. Murayama, Y. Nakayama, K. Yamazaki, Y. Hoshina, H. Watanabe, N. Fuutagawa, H. Kawanishi, T. Uemura, and H. Narui, "Watt-class green (530 nm) and blue (465 nm) laser diodes," *Phys. Status Solidi (A)*, vol. 215, no. 10, May 2018, Art. no. 1700513, doi: [10.1002/pssa.201700513](https://doi.org/10.1002/pssa.201700513).
- [2] K. V. Chellappan, E. Erden, and H. Urey, "Laser-based displays: A review," *Appl. Opt.*, vol. 49, no. 25, p. F79, Sep. 2010, doi: [10.1364/AO.49.000F79](https://doi.org/10.1364/AO.49.000F79).
- [3] A. Humeau-Heurtier, G. Mahe, S. Durand, and P. Abraham, "Multi-scale entropy study of medical laser speckle contrast images," *IEEE Trans. Biomed. Eng.*, vol. 60, no. 3, pp. 872–879, Mar. 2013, doi: [10.1109/TBME.2012.2208642](https://doi.org/10.1109/TBME.2012.2208642).
- [4] J. W. Goodman, "Some fundamental properties of speckle," *J. Opt. Soc. Amer.*, vol. 66, no. 11, pp. 1145–1150, Nov. 1976, doi: [10.1364/JOSA.66.001145](https://doi.org/10.1364/JOSA.66.001145).
- [5] J. W. Goodman, "Speckle in optical projection displays," in *Speckle Phenomena in Optics: Theory and Applications*, J. W. Goodman, Ed. Englewood, CO, USA: Roberts Company, 2006, pp. 203–228.
- [6] J. Kinoshita, H. Aizawa, A. Takamori, K. Yamamoto, H. Murata, and K. Tojo, "Angular dependence of screen speckle and fiber speckle of coupled output of nine high-power blue laser diodes through a multimode fiber," *Opt. Rev.*, vol. 23, no. 1, pp. 121–132, Feb. 2016, doi: [10.1007/s10043-015-0150-1](https://doi.org/10.1007/s10043-015-0150-1).
- [7] N. E. Yu, J. W. Choi, H. Kang, D. K. Ko, S. H. Fu, and J. W. Liou, "Speckle noise reduction on a laser projection display via a broadband green light source," *Opt. Exp.*, vol. 22, no. 3, pp. 3547–3556, 2014, doi: [10.1364/OE.22.003547](https://doi.org/10.1364/OE.22.003547).
- [8] D. Halpaap, M. Marconi, R. Hernandez, A. M. Yacomotti, J. Tiana-Alsina, and C. Masoller, "Experimental study of speckle patterns generated by low-coherence semiconductor laser light," *Chaos: Interdiscipl. J. Nonlinear Sci.*, vol. 30, no. 6, Jun. 2020, Art. no. 063147, doi: [10.1063/5.0006007](https://doi.org/10.1063/5.0006007).
- [9] Z. Tong and X. Chen, "Speckle contrast for superposed speckle patterns created by rotating the orientation of laser polarization," *J. Opt. Soc. Amer. A, Opt. Image Sci.*, vol. 29, no. 10, pp. 2074–2079, 2012, doi: [10.1364/JOSAA.29.002074](https://doi.org/10.1364/JOSAA.29.002074).
- [10] L. Wang, T. Tschudi, T. Halldorsson, and P. R. Petursson, "Speckle reduction in laser projection systems by diffractive optical elements," *Appl. Opt.*, vol. 37, no. 10, pp. 1770–1775, 1998, doi: [10.1364/AO.37.001770](https://doi.org/10.1364/AO.37.001770).
- [11] V. Kumar, K. Usmani, V. Singh, A. K. Dubey, M. Gupta, and D. S. Mehta, "Laser speckle reduction using spatially structured and temporally varying beams using double diffractive optical elements," *Laser Phys. Lett.*, vol. 17, no. 3, Feb. 2020, Art. no. 036003, doi: [10.1088/1612-202X/ab723a](https://doi.org/10.1088/1612-202X/ab723a).
- [12] S. Kubota and J. W. Goodman, "Very efficient speckle contrast reduction realized by moving diffuser device," *Appl. Opt.*, vol. 49, no. 23, pp. 4385–4391, 2010, doi: [10.1364/AO.49.004385](https://doi.org/10.1364/AO.49.004385).
- [13] V. Kumar, M. Gupta, A. K. Dubey, S. Tayal, V. Singh, and D. S. Mehta, "Design and development of laser speckle reduction device using waveguide diffuser and pyramidal cavity for projection imaging," *J. Opt.*, vol. 22, no. 11, Nov. 2020, Art. no. 115601, doi: [10.1088/2040-8986/abb41b](https://doi.org/10.1088/2040-8986/abb41b).
- [14] J. Manni and J. Goodman, "Versatile method for achieving 1% speckle contrast in large-venue laser projection displays using a stationary multimode optical fiber," *Opt. Exp.*, vol. 20, pp. 11288–11315, May 2012, doi: [10.1364/OE.20.011288](https://doi.org/10.1364/OE.20.011288).
- [15] M. Sun, "Speckle suppression with a rotating light pipe," *Opt. Eng.*, vol. 49, no. 2, Feb. 2010, Art. no. 024202, doi: [10.1117/1.3314310](https://doi.org/10.1117/1.3314310).
- [16] Z. Tong, C. Sun, Y. Ma, M. Wang, S. Jia, and X. Chen, "Laser spatial coherence suppression with refractive optical elements toward the improvement of speckle reduction by light pipes," *IEEE Access*, vol. 7, pp. 172190–172198, Nov. 2019, doi: [10.1109/ACCESS.2019.2956517](https://doi.org/10.1109/ACCESS.2019.2956517).
- [17] R. Ma, Y. J. Rao, W. L. Zhang, and B. Hu, "Multimode random fiber laser for speckle-free imaging," *IEEE J. Sel. Topics Quantum Electron.*, vol. 25, no. 1, pp. 1–6, Jan. 2019, doi: [10.1109/JSTQE.2018.2833472](https://doi.org/10.1109/JSTQE.2018.2833472).
- [18] R. Ma, W. L. Zhang, J. Y. Guo, and Y. J. Rao, "Decoherence of fiber supercontinuum light source for speckle-free imaging," *Opt. Exp.*, vol. 26, no. 20, pp. 26758–26765, Oct. 2018, doi: [10.1364/OE.26.026758](https://doi.org/10.1364/OE.26.026758).
- [19] S. C. Shin, S. S. Yoo, S. Y. Lee, C.-Y. Park, S.-Y. Park, J. W. Kwon, and S.-G. Lee, "Removal of hot spot speckle on laser projection screen using both the running screen and the rotating diffuser," *Displays*, vol. 27, no. 3, pp. 91–96, Jul. 2006, doi: [10.1016/j.displa.2005.12.002](https://doi.org/10.1016/j.displa.2005.12.002).
- [20] A. Lapchuk, G. A. Pashkevich, O. V. Prygun, V. Yurlov, Y. Borodin, A. Kryuchyn, A. A. Korchovi, and S. Shylo, "Experiment evaluation of speckle suppression efficiency of 2D quasi-spiral M-sequence-based diffractive optical element," *Appl. Opt.*, vol. 54, no. 28, p. E47, Oct. 2015, doi: [10.1364/ao.54.000e47](https://doi.org/10.1364/ao.54.000e47).
- [21] C.-Y. Chen, W.-C. Su, C.-H. Lin, M.-D. Ke, Q.-L. Deng, and K.-Y. Chiu, "Reduction of speckles and distortion in projection system by using a rotating diffuser," *Opt. Rev.*, vol. 19, no. 6, pp. 440–443, Nov. 2012, doi: [10.1007/s10043-012-0075-x](https://doi.org/10.1007/s10043-012-0075-x).
- [22] D. Mehta, D. Naik, R. K. Singh, and M. Takeda, "Laser speckle reduction by multimode optical fiber bundle with combined temporal, spatial, and angular diversity," *Appl. Opt.*, vol. 51, pp. 1894–1904, Apr. 2012, doi: [10.1364/AO.51.001894](https://doi.org/10.1364/AO.51.001894).
- [23] W.-S. Ha, S.-J. Lee, K.-H. Oh, Y.-M. Jung, and J.-K. Kim, "Speckle reduction in near-field image of multimode fiber with a piezoelectric transducer," *J. Opt. Soc. Korea*, vol. 12, no. 3, pp. 126–130, Sep. 2008, doi: [10.3807/JOSK.2008.12.3.126](https://doi.org/10.3807/JOSK.2008.12.3.126).
- [24] W. Ha, S. Lee, Y. Jung, J. K. Kim, and K. Oh, "Acousto-optic control of speckle contrast in multimode fibers with a cylindrical piezoelectric transducer oscillating in the radial direction," *Opt. Exp.*, vol. 17, pp. 17536–17546, Sep. 2009, doi: [10.1364/OE.17.017536](https://doi.org/10.1364/OE.17.017536).
- [25] S. Mingjie and L. Zukang, "Study of speckle suppression by a moving diffuser in liquid crystal on silicon based laser projection system," *Chin. J. Lasers*, vol. 37, no. 3, pp. 718–721, 2010, doi: [10.3788/CJL20103703.0718](https://doi.org/10.3788/CJL20103703.0718).
- [26] Z. Jian, Z. Tong, Y. Ma, M. Wang, S. Jia, and X. Chen, "Laser beam modulation with a fast focus tunable lens for speckle reduction in laser projection displays," *Opt. Lasers Eng.*, vol. 126, Mar. 2020, Art. no. 105918, doi: [10.1016/j.optlaseng.2019.105918](https://doi.org/10.1016/j.optlaseng.2019.105918).
- [27] C.-K. Lo and J.-W. Pan, "Speckle reduction with fast electrically tunable lens and holographic diffusers in a laser projector," *Opt. Commun.*, vol. 454, Jan. 2020, Art. no. 124301, doi: [10.1016/j.optcom.2019.07.063](https://doi.org/10.1016/j.optcom.2019.07.063).
- [28] L. Deng, T. Dong, Y. Fang, Y. Yang, C. Gu, H. Ming, and L. Xu, "Speckle reduction in laser projection based on a rotating ball lens," *Opt. Laser Technol.*, vol. 135, Mar. 2021, Art. no. 106686, doi: [10.1016/j.optlastec.2020.106686](https://doi.org/10.1016/j.optlastec.2020.106686).
- [29] A. Lapchuk, I. Gorbov, Z. Le, Q. Xiong, Z. Lu, O. Prygun, and A. Pankratova, "Experimental demonstration of a flexible DOE loop with wideband speckle suppression for laser pico-projectors," *Opt. Exp.*, vol. 26, no. 20, p. 26188, Oct. 2018, doi: [10.1364/OE.26.026188](https://doi.org/10.1364/OE.26.026188).
- [30] Z. Le, A. Lapchuk, I. Gorbov, Z. Lu, S. Yao, I. Kosyak, T. Kliuieva, Y. Guo, and O. Prygun, "Theory and experiments based on tracked moving flexible DOE loops for speckle suppression in compact laser projection," *Opt. Lasers Eng.*, vol. 124, Jan. 2020, Art. no. 105845, doi: [10.1016/j.optlaseng.2019.105845](https://doi.org/10.1016/j.optlaseng.2019.105845).

- [31] P. J. Kajenski, P. L. Fuhr, and D. R. Huston, "Mode coupling and phase modulation in vibrating waveguides," *J. Lightw. Technol.*, vol. 10, no. 9, pp. 1297–1301, Sep. 1992, doi: [10.1109/50.156882](https://doi.org/10.1109/50.156882).
- [32] V. Yurlov, A. Lapchuk, K. Han, S.-J. Son, B. H. Kim, and N. E. Yu, "Binary code DOE optimization for speckle suppression in a laser display," *Appl. Opt.*, vol. 57, no. 30, p. 8851, Oct. 2018, doi: [10.1364/AO.57.008851](https://doi.org/10.1364/AO.57.008851).
- [33] V. Yurlov, A. Lapchuk, S. Yun, J. Song, and H. Yang, "Speckle suppression in scanning laser display," *Appl. Opt.*, vol. 47, no. 2, pp. 179–187, Jan. 2008, doi: [10.1364/ao.47.000179](https://doi.org/10.1364/ao.47.000179).
- [34] A. Lapchuk, K. Andriy, V. Petrov, V. Yurlov, and V. Klymenko, "Full speckle suppression in laser projectors using two Barker code-type diffractive optical elements," *J. Opt. Soc. Amer. A, Opt. Image Sci.*, vol. 30, no. 1, pp. 22–31, Mar. 2013, doi: [10.1364/JOSAA.30.000022](https://doi.org/10.1364/JOSAA.30.000022).
- [35] J. Zhou, Z. Le, and A. Lapchuk, "Impact of structure and system parameters for speckle suppression in laser pico-projectors based on the tracked moving flexible DOE loop," *Opt. Commun.*, vol. 475, Nov. 2020, Art. no. 126205, doi: [10.1016/j.optcom.2020.126205](https://doi.org/10.1016/j.optcom.2020.126205).
- [36] Q. Gao, Z. Tong, Y. Ma, M. Wang, S. Jia, and X. Chen, "Flexible and lightweight speckle noise suppression module based on generation of dynamic speckles with multimode fiber and macro fiber composite," *Opt. Laser Technol.*, vol. 123, Mar. 2020, Art. no. 105941, doi: [10.1016/j.optlastec.2019.105941](https://doi.org/10.1016/j.optlastec.2019.105941).
- [37] Z. Tong, W. Shen, S. Song, W. Cheng, Z. Cai, Y. Ma, L. Wei, W. Ma, L. Xiao, S. Jia, and X. Chen, "Combination of micro-scanning mirrors and multi-mode fibers for speckle reduction in high lumen laser projector applications," *Opt. Exp.*, vol. 25, no. 4, p. 3795, Feb. 2017, doi: [10.1364/OE.25.003795](https://doi.org/10.1364/OE.25.003795).
- [38] B. Redding, G. Allen, E. Dufresne, and H. Cao, "Low-loss high-speed speckle reduction using a colloidal dispersion," *Appl. Opt.*, vol. 52, no. 6, pp. 1168–1172, Feb. 2013, doi: [10.1364/AO.52.001168](https://doi.org/10.1364/AO.52.001168).
- [39] Y. Yuan, Y. Bi, M. Y. Sun, D. Z. Wang, D. D. Wang, W. N. Gao, and S. Zhang, "Speckle evaluation in laser display: From speckle contrast to speckle influence degree," *Opt. Commun.*, vol. 454, Jan. 2020, Art. no. 124405, doi: [10.1016/j.optcom.2019.124405](https://doi.org/10.1016/j.optcom.2019.124405).
- [40] I. Kompanets and N. Zalyapin, "Methods and devices of speckle-noise suppression (Review)," *Opt. Photon. J.*, vol. 10, no. 10, pp. 219–250, 2020, doi: [10.4236/opj.2020.1010023](https://doi.org/10.4236/opj.2020.1010023).



**ZONGSHEN LIU** received the B.E. degree from the Zhejiang University of Technology, China, in 2019, where he is currently pursuing the M.E. degree in optical engineering. His current research interest includes laser projection displays.



**YANXIN DAI** received the B.S. degree from Henan Polytechnic University, China, in 2017. He is currently pursuing the M.E. degree in optical engineering with the Zhejiang University of Technology, China. His current research interest includes laser projection displays.



**YANYU GUO** received the B.E. degree from the Zhejiang University of Technology, China, in 2018, where she is currently pursuing the M.E. degree in optical engineering. Her current research interest includes laser projection displays.



**JIAYU DENG** received the B.E. degree from the Zhejiang University of Technology, China, in 2018, where he is currently pursuing the M.E. degree in optical engineering. His current research interests include laser projection displays and computer-generated holograms.



**JIAPAO LI** received the B.S. degree from the Zhejiang University of Technology, China, in 2018, where he is currently pursuing the M.E. degree in optical engineering. His current research interest includes laser projection systems.

...



**JUN ZHOU** received the M.E. degree in optical engineering from the Shanghai Institute of Optics and Fine Mechanics, China, in 2013. He is currently pursuing the Ph.D. degree in control science and engineering from the Zhejiang University of Technology, China. His current research interests include laser projection displays and fiber optics.



**ZICHUN LE** received the Ph.D. degree in optical engineering from the Changchun Institute of Optics, Fine Mechanics and Physics, in 1997. She worked with Oxford University, England; the University of Bielefeld, Germany; the University of Iowa, USA; and Chonnam National University. She is currently a Second-Grade Professor with the Zhejiang University of Technology. She is also the Director of the Joint International Research Laboratory of Optoelectronic Information Technology of Zhejiang Province and the Head of the Department of Optical Engineering. She has rich international cooperative researching experience. She is the author of more than 100 scientific works, including five monographs and more than 50 patents. Her current research interests include optics and photonics, optical communications, and signal processing.